LAWRENCE
LIVERMORE
NATIONAL
LABORATORY

LLNL-JRNL-408807

Hydrogen Production by a Hyperthermophilic Membrane-Bound Hydrogenase in Soluble Nanolipoprotein Particles

S. E. Baker, R. C. Hopkins, C. Blanchette, V. Walsworth, R. Sumbad, N. Fischer, E. Kuhn, M. Coleman, B. Chromy, S. Letant, P. Hoeprich, M. W. W. Adams, P. T. Henderson

November 18, 2008

Journal of the American Chemical Society

Hydrogen Production by a Hyperthermophilic Membrane-Bound Hydrogenase in Soluble Nanolipoprotein Particles

Sarah E. Baker, Robert C. Hopkins*, Craig D. Blanchette, Vicki L. Walsworth, Rhoda Sumbad Nicholas O. Fischer, Edward A. Kuhn, Matt Coleman, Brett A. Chromy, Sonia E. Létant, Paul D. Hoeprich[†], Michael W. W. Adams, and Paul T. Henderson[‡].*

Department of Biochemistry, University of Georgia and Physical and Life Sciences Directorate, Lawrence Livermore National Laboratory

To whom correspondence should be addressed. [†]Email: hoeprich2@llnl.gov, [‡]paul.henderson@ucdmc.ucdavis.edu

*These authors contributed equally.

Hydrogenases constitute a promising class of enzymes for *ex vivo* hydrogen production. Implementation of such applications is currently hindered by oxygen sensitivity and, in the case of membrane-bound hydrogenases (MBH), poor water solubility. Nanolipoprotein particles (NLPs), formed from apolipoproteins and phospholipids, offer a novel means to incorporate MBH into in a well-defined water-soluble matrix that maintains the enzymatic activity and is amenable to incorporation into more complex architectures. We report the synthesis, hydrogen-evolving activity and physical

characterization of the first MBH-NLP assembly. This may ultimately lead to the development of biomimetic hydrogen production devices.

Membrane proteins play a key role in the transport of energy across cellular boundaries. Recently, several membrane proteins have been identified as attractive candidates for enabling the conversion of biomass and/or solar energy to renewable fuels.[1-5] Among these promising enzymes are membrane-bound hydrogenases (MBH), which are microbial metalloenzymes that catalyze the reversible reduction of protons to hydrogen using organic matter and/or light as energy sources *in vivo*.

Biocatalysts such as MBH have the potential to enable commercially viable production of hydrogen from renewable resources, such as plant biomass. Hydrogen is a high energy density, potentially zero-pollution transportation fuel and is therefore an extremely attractive candidate fuel for a future carbon-neutral transportation system if it can be produced using renewable resources. Standard inorganic catalysts for conversion of biomass to hydrogen have low selectivities, require extremely high temperatures, are not abundant enough to satisfy a global need, and can be costly.[6]

Hydrogenases are attractive candidates for *ex vivo* biocatalysis because they have catalytic turnover rates several orders of magnitude higher than advanced inorganic catalysts.[7] Because they eliminate competing cellular processes which utilize hydrogen as an energy source, *ex vivo* solution-phase synthetic enzymatic reactions have been shown to produce nearly theoretical yields of hydrogen from glucose or starch.[6, 8, 9] The *ex vivo* strategy for biocatalytic hydrogen production will be significantly improved when oxygen-stable, active hydrogenases (and other enzymes involved in conversion of biomass to hydrogen) can be immobilized on surfaces for reactant cycling and to prevent catalyst poisoning from reaction byproducts.[8, 10]

Hydrogenases can be cytoplasmic or membrane-bound, and are broadly divided into two classes according to the transition metals coordinated at the active site. While the [FeFe]-hydrogenases generally catalyze hydrogen production *in vivo* (as opposed to the reverse reaction, hydrogen oxidation to protons), they are extremely oxygen sensitive.[1] In contrast, the [NiFe]-hydrogenases are more stable to oxygen exposure compared to those with [FeFe] active sites, but preferentially catalyze proton production from hydrogen, thus limiting hydrogen production activity in the presence of trace amounts of molecular hydrogen.[1]

In contrast, MBH from the hyperthermophile *Pyrococcus furiosus,* a microorganism that grows optimally at 100 °C, is advantageous for *ex vivo* hydrogen production. Even though it is the oxygen-resistant [Ni/Fe] type of hydrogenase, it has a 2000-fold greater propensity for catalyzing hydrogen production compared to the reverse reaction.[11] Importantly, MBH retains a significant fraction of initial activity in air over several days, and eventual oxidation of the active site can be reversed using reducing agents or excess hydrogen.[12] For these reasons, MBH from *P. furiosus* is an extremely attractive candidate for bioenergy applications. However, the hydrogenase is associated with the water insoluble *P.furiosus* cell membrane, and several practical challenges, including solubilization of the enzyme while maintaining activity, must be overcome to enable the use of MBH either in the solution phase or immobilized on surfaces for heterogeneous catalysis.

Incorporating MBH into NLPs offers a solution to the problems associated with manipulating and utilizing MBH in crude membrane preparations. NLPs are discoidal nanoparticles formed when an apolipoprotein "scaffold protein" directs the self-assembly of a population of phospholipids into nanoscale lipid bilayers in an aqueous environment[13] (Figure 1). These bilayers closely mimic the cell membrane, allowing membrane proteins to be incorporated and functional inside the nanoparticles.[14] The NLP scaffold protein provides a handle for the eventual immobilization of the enzyme on surfaces[15] for heterogenous catalysis. Additionally, the presence of the scaffold protein constrains the dimensions of the bilayer and ensures quantized, controllable[16, 17] NLP particle size distributions which are stable and consistent between preparations compared to other model membrane systems, such as inverted vesicles and detergent micelles. For example, artificial vesicles are largely insoluble, and structurally unstable. Furthermore, because vesicles are spherical and therefore contain both an exposed and buried leaflet, a large fraction of the enzymes of interest will have active sites buried inside the vesicle.

Detergent micelles do not typically retain the activity of the native membrane protein. NLPs have been successfully used to study a diverse set of solubilized integral membrane proteins in their native environment, including cytochrome P450s, bacterial chemoreceptors, and β_2 adrenergic receptors.[18-20]

Here we report the first successful demonstration of biocatalysis by a bioenergy-related membrane protein incorporated into NLPs. Synthesis of NLPs in the presence of MBH-containing *P. furiosus* membranes enabled incorporation of the MBH into the NLPs, and thus solubilization of the active MBH in aqueous solution.

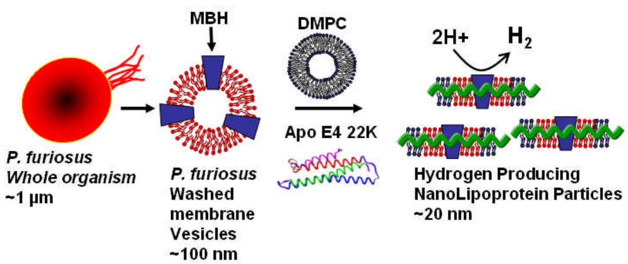

Figure 1. Overview of the process for generating NLPs incorporating membrane hydrogenase from P. furiosus. The cell membrane is first lysed, separated, and washed using centrifugation. Self-assembly of NLPs containing membrane hydrogenase activity is initiated when the P. furiosus washed membranes are incubated with synthetic lipid (DMPC), scaffold protein Apo E4 22K, and surfactant.

Figure 1 provides an overview of the process used to assemble MBH-NLPs: *P. furiosus* cells were lysed and cellular membranes were separated and washed using centrifugation, forming insoluble membrane fragments and vesicles. The scaffold protein used was a truncated helical amphiphilic apoliprotein E with a mass of 22 kD (Apo E422k). A suspension of the membrane fragments was added to synthetic phopsholipid 1,2-Dimyristoyl-*sn*-Glycero-3-Phosphocholine (DMPC), Apo E422k and cholate, a surfactant, using a cholate concentration above the critical micelle concentration (20 mM). The components were thermally cycled above and below the transition temperature of DMPC, followed by removal of excess DMPC and cholate by dialysis against buffer. The particles were then separated from unincorporated free proteins and lipids using size exclusion chromatography (SEC) and the resulting fractions were characterized for size and homogeneity by native and denaturing gel electrophoresis and atomic force microscopy (AFM). The resulting MBH-NLPs were tested for hydrogen production using an established gas chromatography (GC) assay.[11]

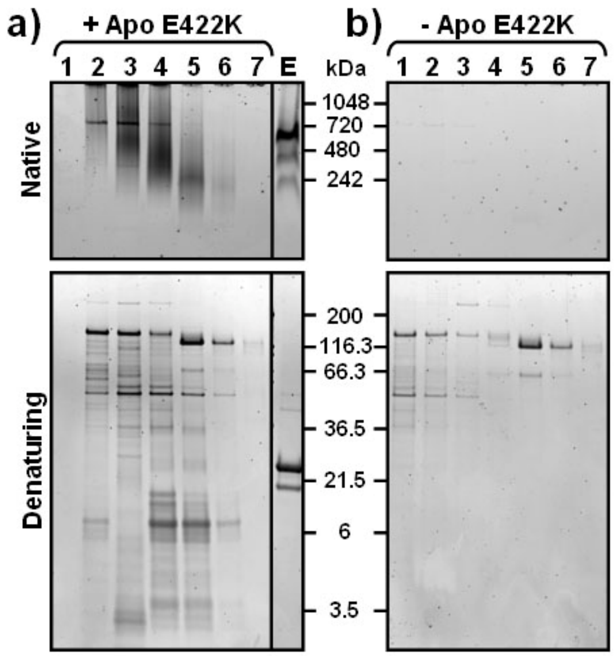

Figure 2. Representative native (top) and denaturing (bottom) polyacrylamide gel electrophoresis of sequential fractions collected after size-exclusion chromatography (SEC) of a) Assembly A: NLP (+scaffold protein) and b) Assembly B: control (- scaffold protein). The lane marked "E" corresponds to an unpurified "empty" NLP assembly, to which no *P. furiosus* membrane was added. The bands in lanes 2-5 in the native gel in a) are characteristic of NLP bands, both according to the molecular weight standards on the gel, as well as the SEC elution time. The native gel in b) contains no NLP bands, consistent with the absence of scaffold protein in the assembly mixture

Figure 2 shows representative native and denaturing polyacrylamide electrophoresis gels loaded with three assemblies. Assembly "A" contained all components required for incorporation of MBH into NLPs: lipid, surfactant, Apo E 422k, and MBH-containing membranes. Assembly "B" excluded the structure-directing scaffold protein, Apo E422k, from the assembly mixture, and therefore served to elucidate the effects of NLP incorporation on MBH solubility, particle size, and hydrogenase activity. Assembly “E” contained “empty” NLPs, which were prepared in the absence of MBH-containing membranes for comparison of particle size distributions to those present in MBH-NLPs.

Figure 2a shows both native (top) and denaturing (bottom) polyacrylamide gels loaded with samples from SEC fractions resulting from MBH-NLP assembly A. Lanes 1-7 are from 1 mL SEC fractions collected at a flow rate of 0.5 mL/minute. Fraction collection began 15 minutes after injection (lane 1). The void volume of the column was 8 mL (16 minutes) using blue dextran as the marker. The broad smears in lanes 2-5 of the native gels are characteristic of NLP complexes. However, fractions 2, 3 and 4 appear to contain particles of *larger* size than the empty NLPs in Lane “E”, consistent with a population of NLPs with *P. furiosus* membrane proteins incorporated into the particles. The corresponding denaturing SDS gel lanes (Figure 2a bottom) show bands consistent with *P. furiosus* membrane proteins, indicating incorporation of *P. furiosus* membrane proteins, including those that contribute to hydrogenase activity, into the NLP-like particles.

Figure 2b shows SEC purification fractions of assembly B, where lanes 1-7 represent the same elution times as those in lanes 1-7 in Figure 2a. The native gel contained only very low intensity bands in fractions 1, 2, and 3 indicating that no significant concentration of particles in the size range of NLPs were present, consistent with the fact that no structure-directing scaffold protein was added. The corresponding denaturing SDS gel shows protein bands consistent with *P. furiosus* membrane proteins in every fraction. Combined, these gel results show that *P. furiosus* membrane proteins were eluted from the SEC column, but not in the form of NLPs. The lower intensity of the bands in Figure 2b may be due in part to sample filtration prior to SEC purification, which removed protein-containing fragments larger than ~200 nm in the assemblies. With no scaffold protein present to break up and solubilize the vesicles, assembly B may have contained insoluble or large particles which were removed during the filtration step. It is important to note that assembly A fractions containing substantial protein content eluted at later times from the SEC column compared to assembly B fractions, and were thus smaller in size. This discrepancy in elution time is another indication that addition of the Apo E422k scaffold protein directed the formation of smaller particles compared to those present in the assembly lacking Apo E422k.

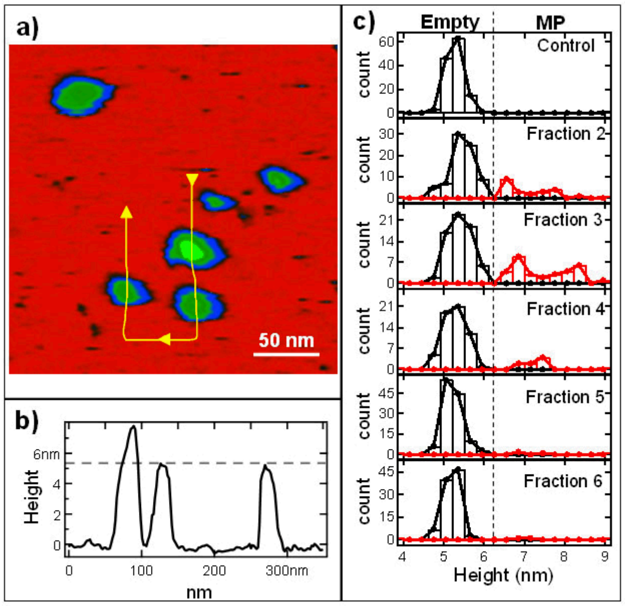

Figure 3. AFM image and analysis of MBH incorporated NLPs. **a)** AFM image of NLPs from fraction 3 in assembly A. Bright green regions are indicative of particles that are higher than 6.5 nm. **b)** Cross section of the three particles with line trace in a), showing height differences between NLPs. **c)** Histogram of heights observed for "empty" NLP (assembled without *P. furiosus* membrane) and size-exclusion fractions 2-6 from Assembly A, assembled with *P. furiosus* membrane. A population of "taller" NLPs (red trace) is observed in Assembly A This population presumably represents membrane associated NLPs.

Gel electrophoresis of the SEC fractions from assembly A support the formation of NLPs containing proteins from the *P. furiosus* crude membranes. In order to determine the morphology and size distribution of these particles, the SEC fractions were characterized with AFM. Figure 3a shows a representative AFM image of fraction 3 from assembly A. Round, discrete disk-shaped particles on the order of 20-30 nm in diameter are observed with varied height profiles. The heights of the particles are depicted as variations in the shade of green in the center of each particle. Cross sections of two representative particles (following the superimposed yellow line) are shown in Figure 3b. As shown by the height profile, the lighter green regions correspond to heights greater than 6.5 nm. Fractions 2, 3, and 4 were found by AFM to consist of nanometer scale discoidal particles with some fraction of the particles determined to be higher than the NLPs in an empty assembly. The height profiles of these fractions are depicted in the histograms of NLP height in Figure 3c. The top histogram represents the height distributions of empty NLPs, displaying a Gaussian distribution with a mean height of 4.9 +/- 0.2 nm, consistent with the height of a lipid bilayer. In contrast, assembly A fractions 2, 3, and 4 contain two populations of NLPs: those which have height profiles very similar to those of the empty NLPs, and a population of particles which have significantly "taller" height profiles than the empty NLP subset. Because *P. furiosus* membranes have associated membrane proteins, including MBH, which can both span and extend beyond the cell membrane, the subset of taller NLPs likely contains MBH.

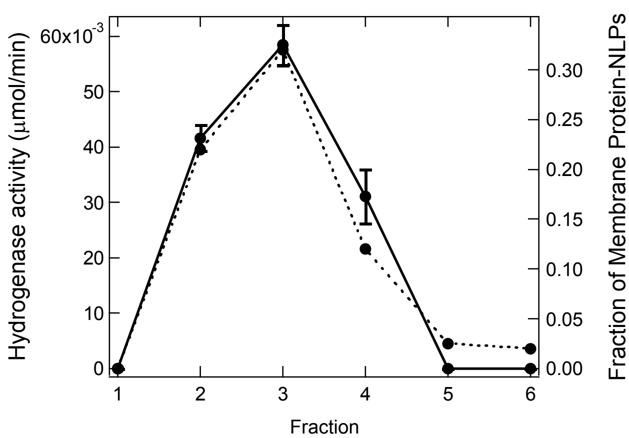

Figure 4. Hydrogenase activity as a function of NLP fraction. The hydrogenase activity (solid line) closely corresponded with the percent of NLPs containing membrane proteins (dotted line), as assessed by AFM. The fraction with the highest percentage of membrane protein associated NLPs (fraction 3) also had the highest level of hydrogenase activity. The total units of hydrogenase activity added to the assembly were 0.09 U (µmol/min/ml). The total units of hydrogenase activity recovered exceeded the initial activity, and were 0.13 U.

Remarkably, the particles in fractions 2, 3, and 4 from assembly A were found to generate hydrogen in the presence of methyl viologen, a non-physiological electron carrier, using sodium dithionite, an electron donor, as determined by GC analysis of the head space above the solution. Figure 4 shows the hydrogen-producing activity of each NLP-containing fraction (left axis), and the corresponding populations of membrane protein-containing NLPs according to AFM (right axis). The amount of hydrogenase activity in each fraction correlated closely with the proportion of apparent *P. furiosus* membrane-protein containing NLPs.

Incorporation of MBH into NLPs both stabilized the enzyme in a soluble form and appeared to preserve the enzymatic activity. The total hydrogenase activity used for the material loaded onto the SEC column for the MBH-NLP assembly was 0.09 U (in µmol/min), and the total hydrogenase activity *recovered* from fractions 2, 3, and 4 totaled 0.13 U: (0.042, 0.058, and 0.031 U, respectively, shown in Figure 4). In contrast, fractions from the assembly B, which lacked scaffold protein, had no measurable hydrogenase activity. The lack of activity from assembly B may be due to denaturation of the MBH by the surfactant present in the NLP assembly solution, which may be irreversible in the absence of a stabilizing scaffold protein, rendering the protein more sensitive to oxygen.

The *ex vivo* use of purified cytoplasmic hydrogenases and other compatible enzymes as components of pathways for hydrogen production have been shown to result in several fold higher yields of hydrogen from glucose or starch than *in vivo* systems, albeit over a limited time scale.[8,9] Hydrogenase stability in the presence of oxygen, and immobilization for eventual continuous processing, are areas requiring further development. We used self-assembled, biomimetic lipid nanoparticles as a tool for both solubilizing and stabilizing a unique membrane-bound hydrogenase enzyme with attractive biocatalytic properties. These properties include reversible and low sensitivity to inactivation by oxygen, extremely high thermal and chemical stability, and a remarkable predilection for hydrogen production as opposed to the competing reverse reaction, hydrogen oxidation, *in vivo*.[21] Incorporation into lipid nanoparticles will enable the MBH to be immobilized on high surface area porous supports for continuous reactant cycling, and to be tested in a solution phase synthetic enzyme pathways for *ex vivo* hydrogen production from biomass.

In this study a crude membrane preparation of the hyperthermophile *P. furiosus* was incorporated into nanolipoprotein particles using a self assembly process. The resulting "filled" particles were morphologically distinct from "empty" NLPs, presumably because of protruding *P. furiosus* transmembrane proteins. Furthermore, the *P. furiosus* membranes incorporated into NLPs were found to approximate the hydrogenase activity of the parent membranes. The degree of activity correlated with the fraction of "tall" NLPs in the mixture. The results indicate that this process can be used to solubilize complex membrane biocatalysts from crude membrane preparations while preserving the initial catalytic activity, opening the door to using membrane proteins as biocatalysts for renewable energy production.

Acknowledgments

The authors are grateful to Drs. Karl Weisgraber and Matt Coleman for providing reagents. This work performed under the auspices of the U.S. Department of Energy by Lawrence Livermore National Laboratory under Contract DE-AC52-07NA27344 with support from Lawrence Livermore National Laboratory (LDRD 06-SI-003 awarded to PDH). RCH and MWWA were supported by a contract (DE-FG02-05ER15710) from the Department of Energy

Supporting Information Available: Experimental details on preparation and characterization of hydrogen producing nanolipoprotein particles.

References

1. Goldet, G.; Wait, A. F.; Cracknell, J. A.; Vincent, K. A.; Ludwig, M.; Lenz, O.; Friedrich, B.; Armstrong, F. A. *Journal of the American Chemical Society* **2008**, 130, (33), 11106-11113.

2. Cracknell, J. A.; Vincent, K. A.; Ludwig, M.; Lenz, O.; Friedrich, B.; Armstrong, F. A. *Journal of the American Chemical Society* **2007**, 130, 424-425.

3. Kovacs, K. L.; Maroti, G.; Rakhely, G. *International Journal of Hydrogen Energy* **2006**, 31, (11), 1460-1468.

4. Ho, D.; Chu, B.; Lee, H.; Brooks, E. K.; Kuo, K.; Montemagno, C. D. *Nanotechnology* **2005**, 16, (12), 3120-3132.

5. Vincent, K. A.; Cracknell, J. A.; Lenz, O.; Zebger, I.; Friederich, B.; Armstrong, F. *Proceedings of the National Academy of Sciences* **2005**, 102, (47), 16951-16954.

6. Zhang, Y.-H. P.; Evans, B. R.; Mielenz, J. R.; Hopkins, R. C.; Adams, M. W. W. *PLoS ONE* **2007**, e456, (5), 1-6.

7. Sanderson, K. *Nature* **2008**, 452, 400-402.

8. Woodward, J.; Mattingly, S. M.; Danson, M.; Hough, D.; Ward, N.; Adams, M. *Nature Biotechnology* **1996**, 14, 872-874.

9. Woodward, J.; Orr, M.; Cordray, K.; Greenbaum, E. *Nature* **2000**, 405, 1014-1015.

10. Elgren, T. E.; Zadvorny, O. A.; Brecht, E.; Douglas, T.; Zorin, N. A.; Maroney, M. J.; Peters, J. W. *Nano Letters* **2005**, 5, (10), 2085-2087.

11. Sapra, R.; Bagramyan, K.; Adams, M. W. W. *Proceedings of the National Academy of Sciences* **2003**, 100, (13), 7545-7550.

12. Sapra, R.; Verhagen, M. F. J. M.; Adams, M. W. W. *Journal of Bacteriology* **2000**, 182, (12), 3423-3428.

13. Bayburt, T. H.; Grinkova, Y. V.; Sligar, S. G. *Nano Letters* **2002**, 2, (8), 853-856.

14. Bayburt, T. H.; Sligar, S. G. *Protein Science* **2003**, 12, 2476-2481.

15. Borch, J.; Torta, F.; Sligar, S. G.; Roepstorff, P. *Analytical Chemistry* **2008**, 80, (16), 6245-6252.

16. Blanchette, C. D.; Law, R.; Benner, W. H.; Pesavento, J. B.; Cappuccio, J. A.; Walsworth, V. L.; Kuhn, E. A.; Corzette, M.; Chromy, B. A.; Segelke, B. W.; Coleman, M. A.; Bench, G.; Hoeprich, P. D.; Sulcheck, T. A. *Journal of Lipid Research* **2008**, 49, (7), 1420-1430.

17. Chromy, B. A.; Arroyo, E.; Blanchette, C. D.; Bench, G.; Benner, H.; Cappuccio, J. A.; Coleman, M. A.; Henderson, P. T.; Hinz, A. K.; Kuhn, E. A.; Pesavento, J. B.; Segelke, B. W.; Sulcheck, T. A.; Tarasow, T.; Walsworth, V. L.; Hoeprich, P. D. *Journal of the American Chemical Society* **2007**, 129, 14348-14354.

18. Nath, A.; Atkins, W. M.; Sligar, S. G. *Biochemistry* **2007**, 46, (8), 2059-2069.

19. Boldog, T.; Grimme, S.; Li, M.; Sligar, S.; Hazelbauer, G. L. *Proceedings of the National Academy of Sciences* **2006**, 103, (31), 11509-11514.

20. Leitz, A. J.; Bayburt, T. H.; Barnakov, A. N.; Springer, B. A.; Sligar, S. G. *BioTechniques* **2006**, 40, (5), 601-612.

21. Hedderich, R. *Journal of Bioenergetics and Biomembranes* **2004**, 36, (1), 65-75.

TOC Graphic

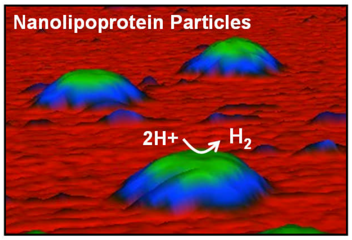
Nanolipoprotein Particles
2H+
H2